

Supplementary information

High-efficiency unbiased water splitting with photoanodes harnessing polycarbazole hole transport layers

Jin Wook Yang,^a Su Geun Ji,^a Chang-Seop Jeong,^b Jaehyun Kim,^a Hee Ryeong Kwon,^a Tae Hyung Lee,^a Sol A Lee,^a Woo Seok Cheon,^a Seokju Lee,^a Hyungsoo Lee,^a Min Sang Kwon,^a Jooho Moon,*^b Jin Young Kim,*^a Ho Won Jang*^{a,c}

^aDepartment of Materials Science and Engineering, Research Institute of Advanced Materials, Seoul National University, Seoul 08826, Republic of Korea

^bDepartment of Materials Science and Engineering, Yonsei University, Seoul 03722, Republic of Korea

^cAdvanced Institute of Convergence Technology, Seoul National University, Suwon 16229, Republic of Korea

*E-mail: jmoon@yonsei.ac.kr; jykim.mse@snu.ac.kr; hwjang@snu.ac.kr

Contents

Fig. S1 Schematic illustration of NiFeCoO_x/CPF-TCB/Mo:BiVO₄ photoanode fabrication process.

Fig. S2 *J-V* curves for electropolymerization of CPF-TCB on Mo:BiVO₄.

Fig. S3 Photographs of fabricated samples.

Fig. S4 (a) Top SEM image of CPF-TCB/Mo:BiVO₄ and EDX mapping of (b) Bi, (c) V, (d) O, (e) C, and (f) N.

Fig. S5 *J-V* curves of CPF-TCB/Mo:BiVO₄ with different thicknesses of CPF-TCB in K-Bi buffer (pH 9.5).

Fig. S6 *J-V* curves of different NiFeCoO_x/CPF-TCB/Mo:BiVO₄ photoanodes manufactured with the same process.

Fig. S7 Top SEM images of NiFeCoO_x/CPF-TCB/Mo:BiVO₄ (a) before and (b) after the LSV measurement.

Fig. S8 Fourier transformed V *K*-edge EXAFS spectra of Mo:BiVO₄ and CPF-TCB/Mo:BiVO₄.

Fig. S9 XPS wide spectra of (a) Mo:BiVO₄, (b) CPF-TCB, and (c) CPF-TCB/Mo:BiVO₄.

Fig. S10 Bi 4f XPS spectra of Mo:BiVO₄ and CPF-TCB/Mo:BiVO₄ with different Ar plasma etching times.

Fig. S11 (a) Ni 2p, (b) Fe 2p, (c) Co 2p, (d) Bi 4f, (e) V 2p, (f) N 1s, (g) C 1s, and (h) O 1s XPS wide spectra of NiFeCoO_x/CPF-TCB/Mo:BiVO₄.

Fig. S12 Optimized structures of CPF-TCB/BiVO₄ in (a) side and (b) top view for DFT calculations.

Fig. S13 Normalized OCP decay profiles of Mo:BiVO₄ and CPF-TCB/Mo:BiVO₄.

Fig. S14 UV-vis Tauc plots and optical band gaps of (a) Mo:BiVO₄ and (b) CPF-TCB. (c) UV-vis spectra of CPF-TCB.

Fig. S15 UPS (a) SEE spectra and (b) VB spectra of Mo:BiVO₄ and CPF-TCB/Mo:BiVO₄.

Fig. S16 (a) Schematic illustration and (b) 3 electrode *J-V* curves of the perovskite photocathode in K-P_i buffer (pH 7).

Fig. S17 (a) Schematic illustration and (b) 2 electrode *J-V* curves of the perovskite/Si tandem solar cell.

Fig. S18 Photographs of (a) PA-PC and (b) PV-PA tandem devices.

Table S1 Series resistances (R_s), charge transport resistances (R_{sc}), charge transfer resistances (R_{ct}), and chi-squared (χ^2) values fitted from EIS curves.

Table S2 Donor densities (N_D) of photoanodes calculated by M-S plots.

Table S3 Fitting parameters and chi-squared (χ^2) values of the TRPL.

Table S4 STH conversion efficiency benchmarks of PA-PC tandem devices in mode T.

Table S5 STH conversion efficiency benchmarks of PV-PA tandem devices in mode T.

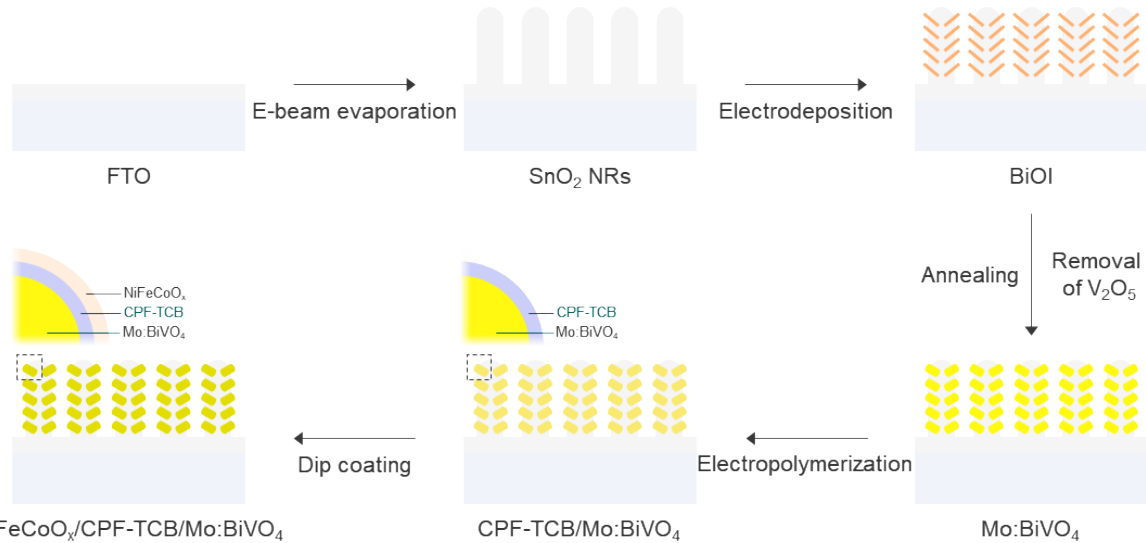


Fig. S1 Schematic illustration of NiFeCoO_x/CPF-TCB/Mo:BiVO₄ photoanode fabrication process.

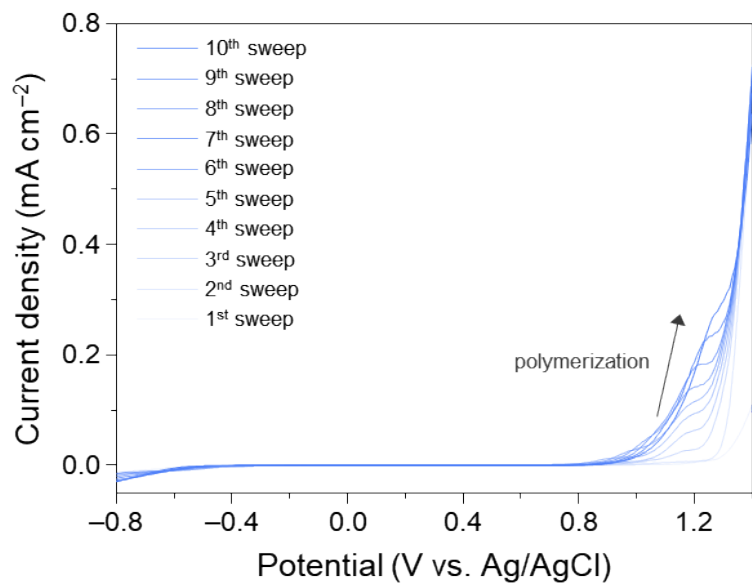


Fig. S2 J - V curves for electropolymerization of CPF-TCB on Mo:BiVO₄.

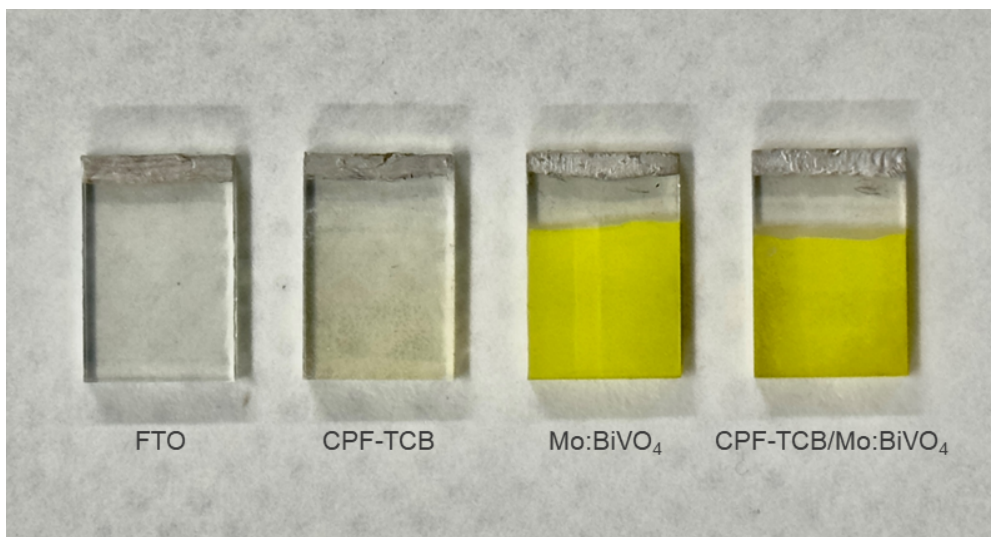


Fig. S3 Photographs of fabricated samples.

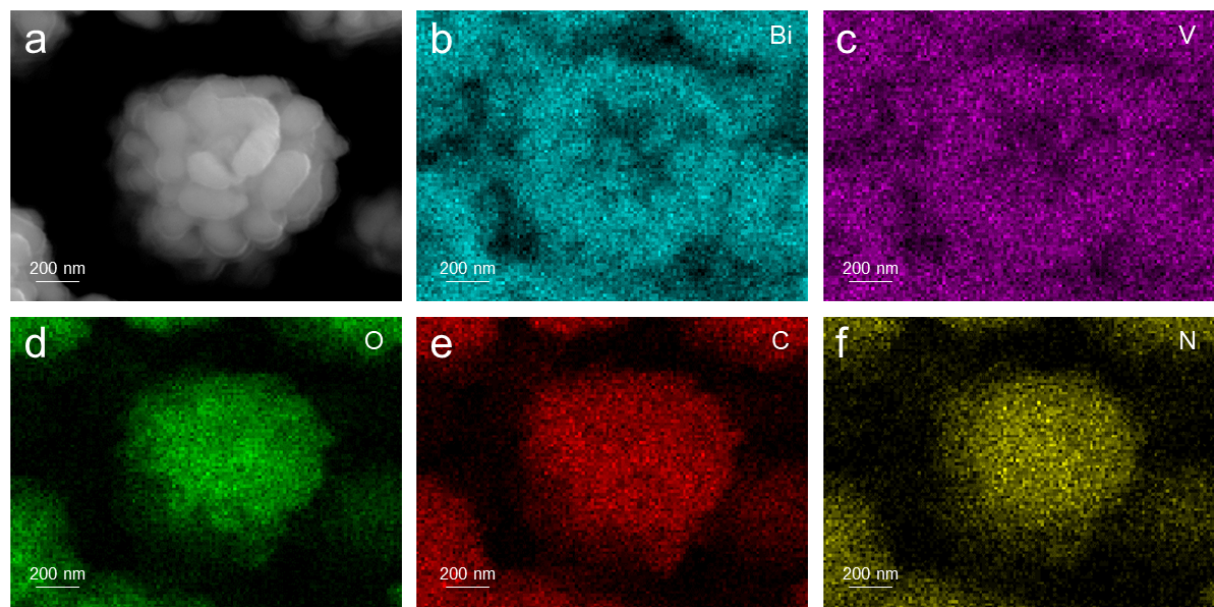


Fig. S4 (a) Top SEM image of CPF-TCB/Mo:BiVO₄ and EDX mapping of (b) Bi, (c) V, (d) O, (e) C, and (f) N.

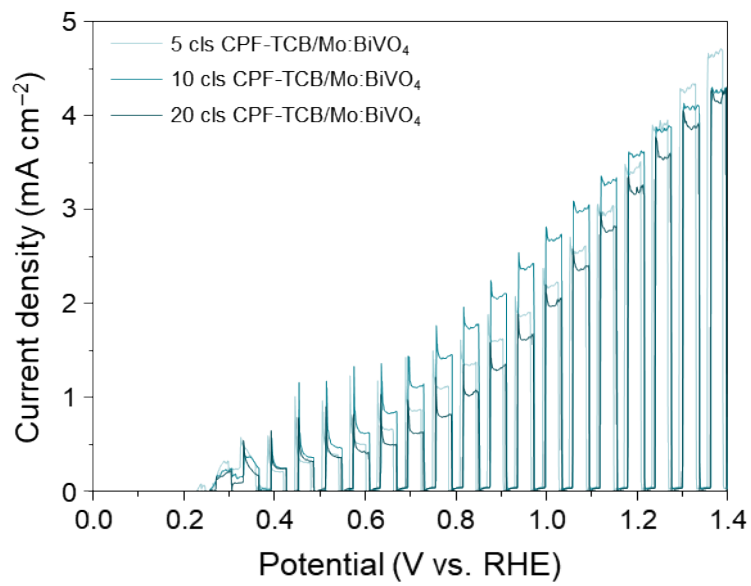


Fig. S5 *J-V* curves of CPF-TCB/Mo:BiVO₄ with different thicknesses of CPF-TCB in K-Bi buffer (pH 9.5).

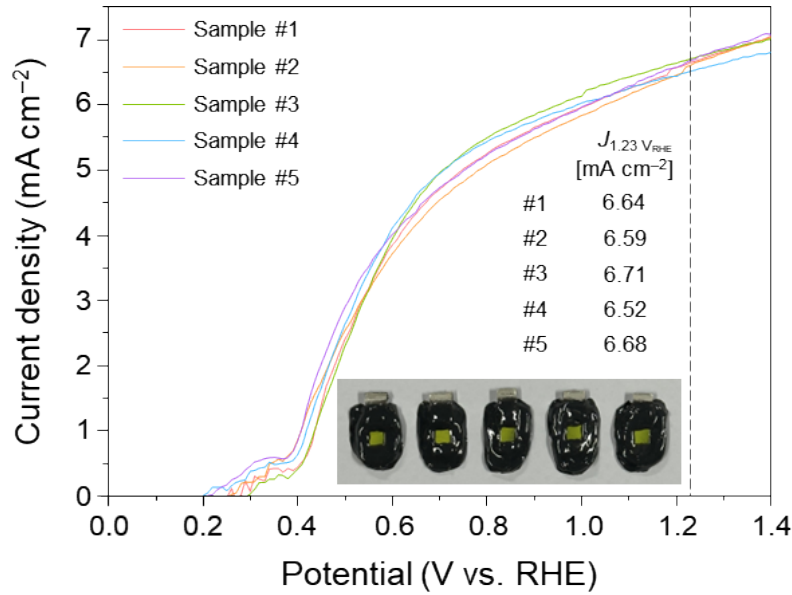


Fig. S6 $J-V$ curves of different NiFeCoO_x/CPF-TCB/Mo:BiVO₄ photoanodes manufactured with the same process.

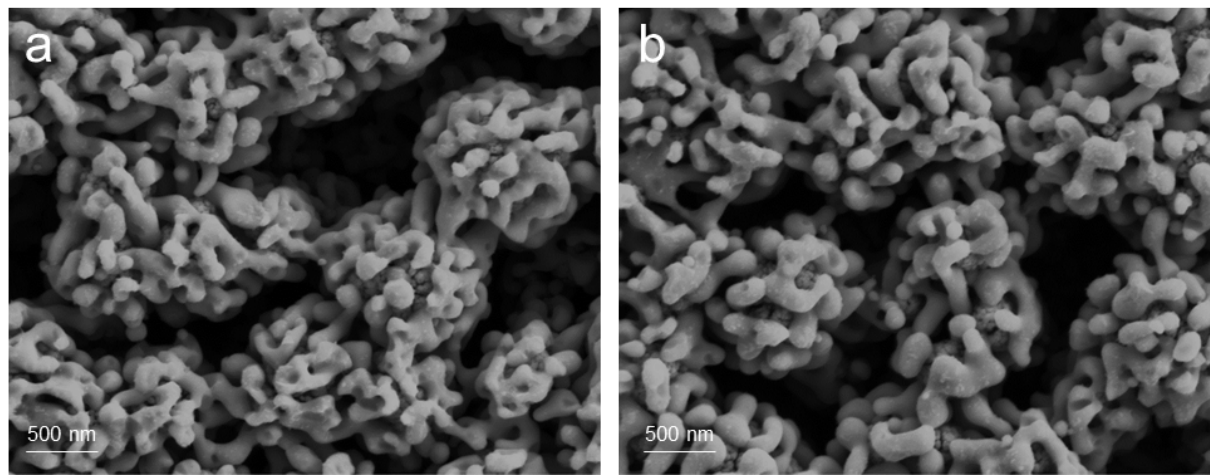


Fig. S7 Top SEM images of $\text{NiFeCoO}_x/\text{CPF-TCB/Mo:BiVO}_4$ (a) before and (b) after the LSV measurement.

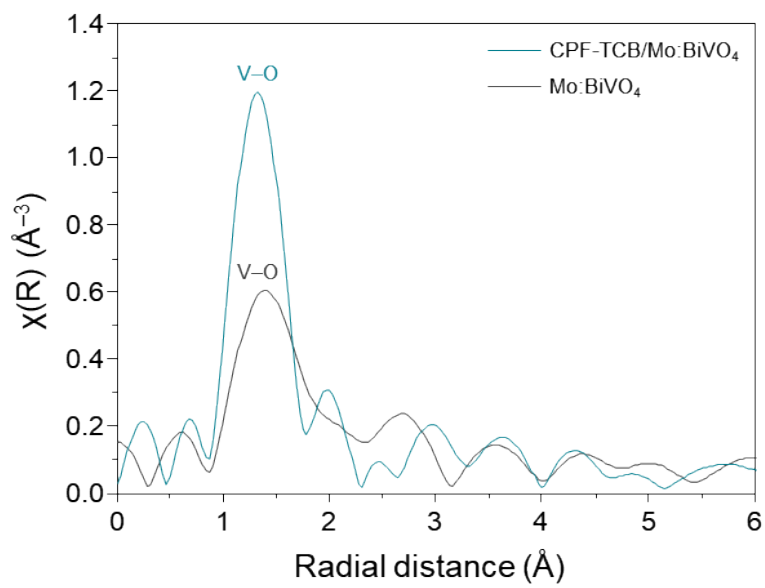


Fig. S8 Fourier transformed V *K*-edge EXAFS spectra of Mo:BiVO₄ and CPF-TCB/Mo:BiVO₄.

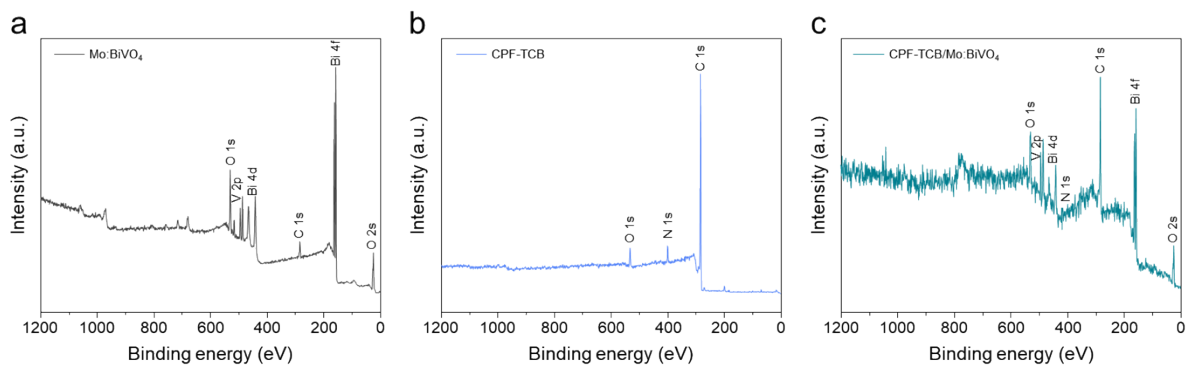


Fig. S9 XPS wide spectra of (a) Mo:BiVO₄, (b) CPF-TCB, and (c) CPF-TCB/Mo:BiVO₄.

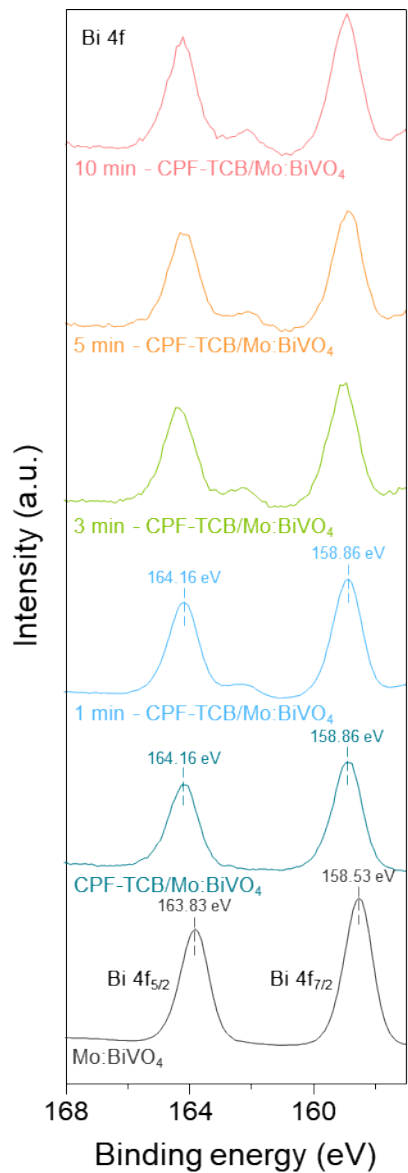


Fig. S10 Bi 4f XPS spectra of Mo:BiVO₄ and CPF-TCB/Mo:BiVO₄ with different Ar plasma etching times.

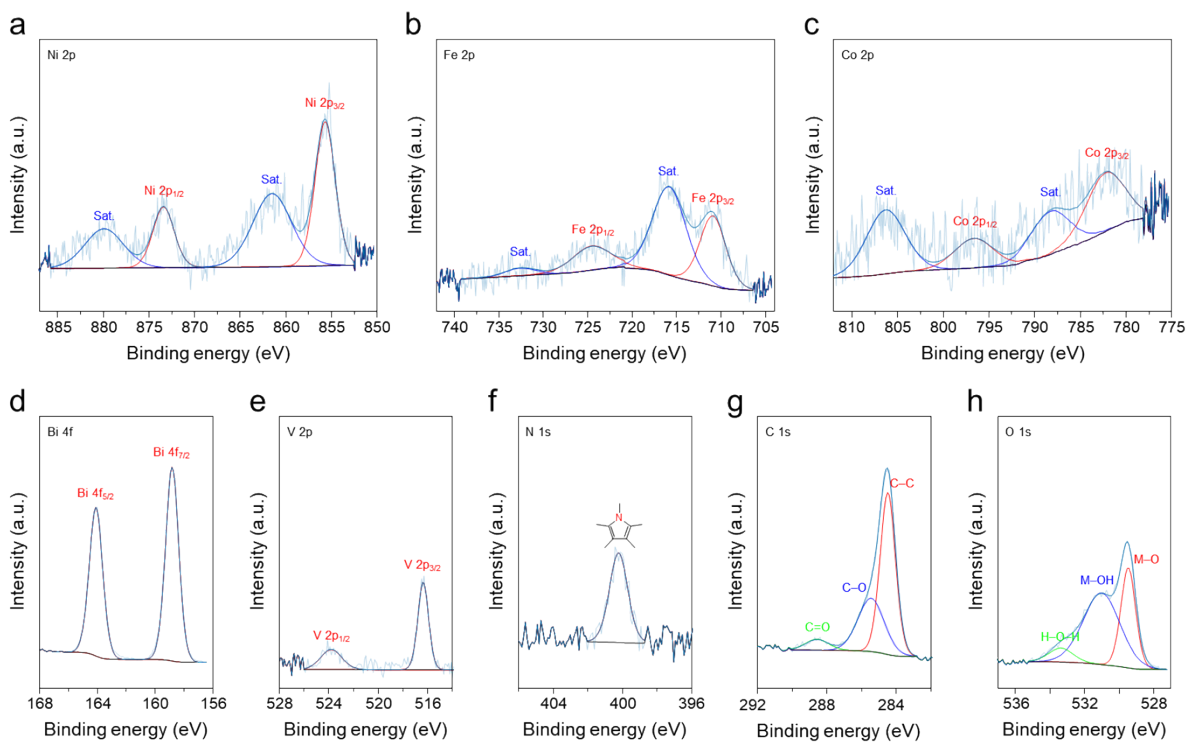


Fig. S11 a) Ni 2p, (b) Fe 2p, (c) Co 2p, (d) Bi 4f, (e) V 2p, (f) N 1s, (g) C 1s, and (h) O 1s XPS spectra of NiFeCoO_x/CPF-TCB/Mo:BiVO₄.

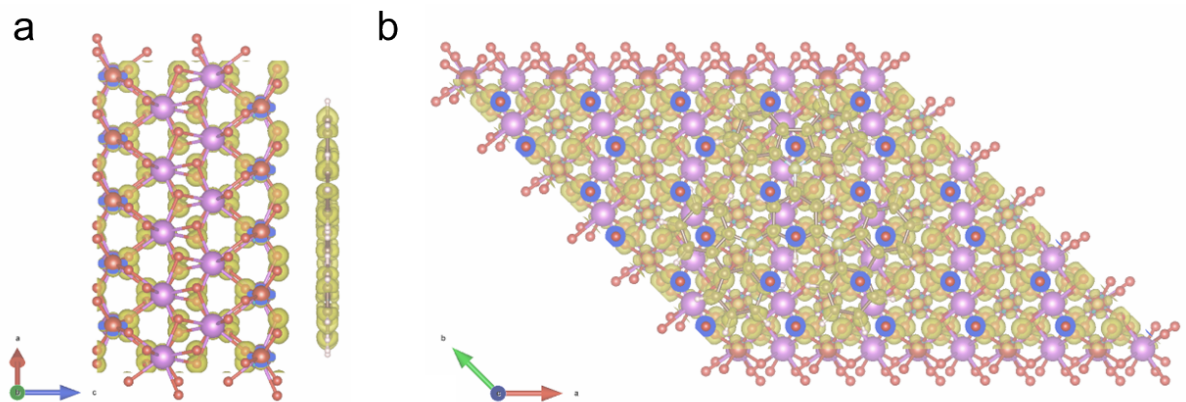


Fig. S12 Optimized structures of CPF-TCB/BiVO₄ in (a) side and (b) top view for DFT calculations.

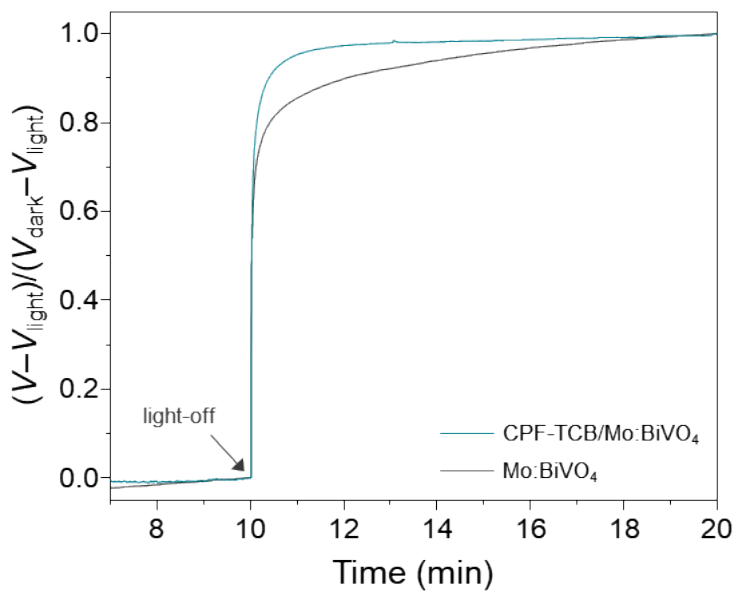


Fig. S13 Normalized OCP decay profiles of Mo:BiVO₄ and CPF-TCB/Mo:BiVO₄.

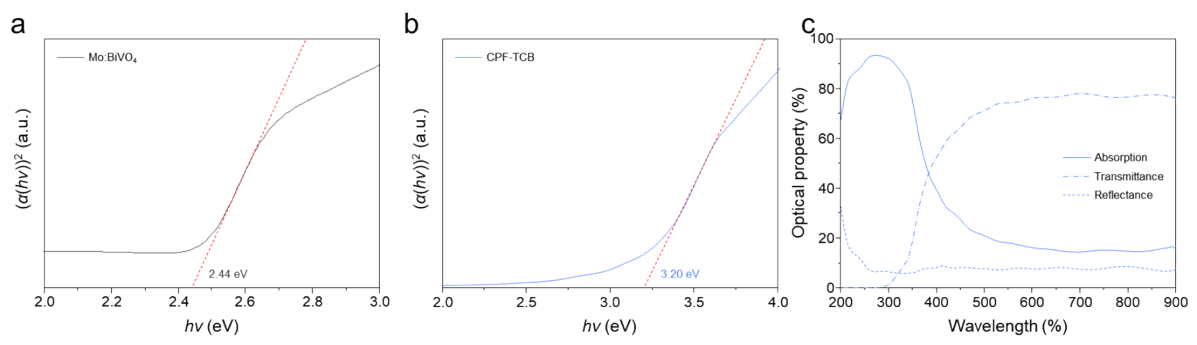


Fig. S14 UV-vis Tauc plots and optical band gaps of (a) Mo:BiVO₄ and (b) CPF-TCB. (c) UV-vis spectra of CPF-TCB.

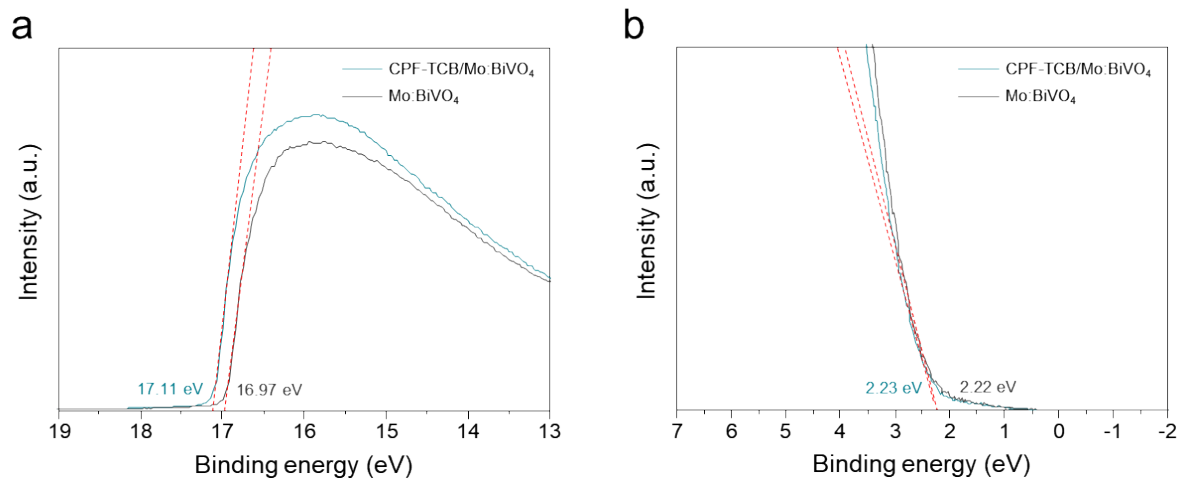


Fig. S15 UPS (a) SEE spectra and (b) VB spectra of Mo:BiVO₄ and CPF-TCB/Mo:BiVO₄.

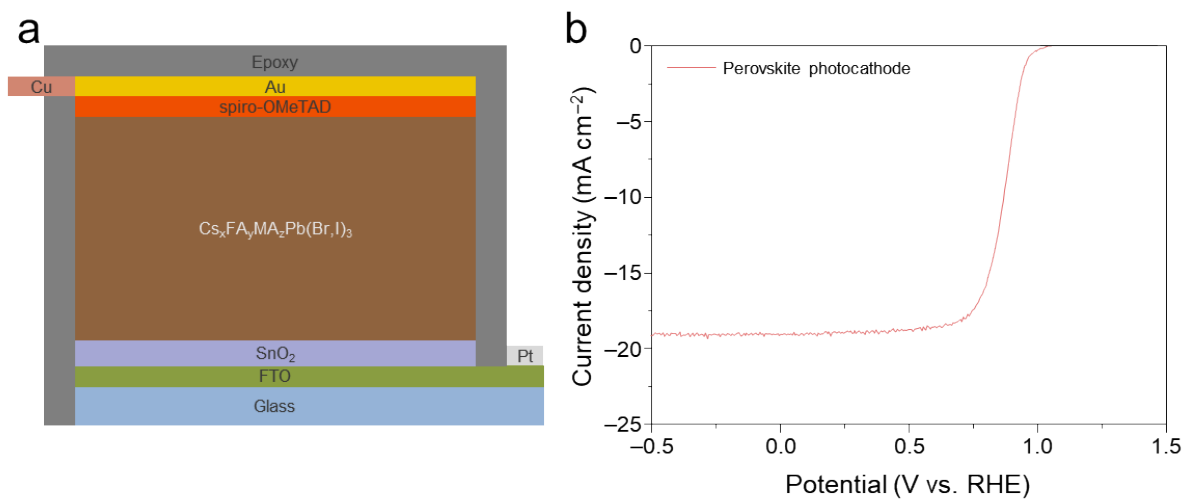


Fig. S16 (a) Schematic illustration and (b) 3 electrode J - V curves of the perovskite photocathode in K-P_i buffer (pH 7).

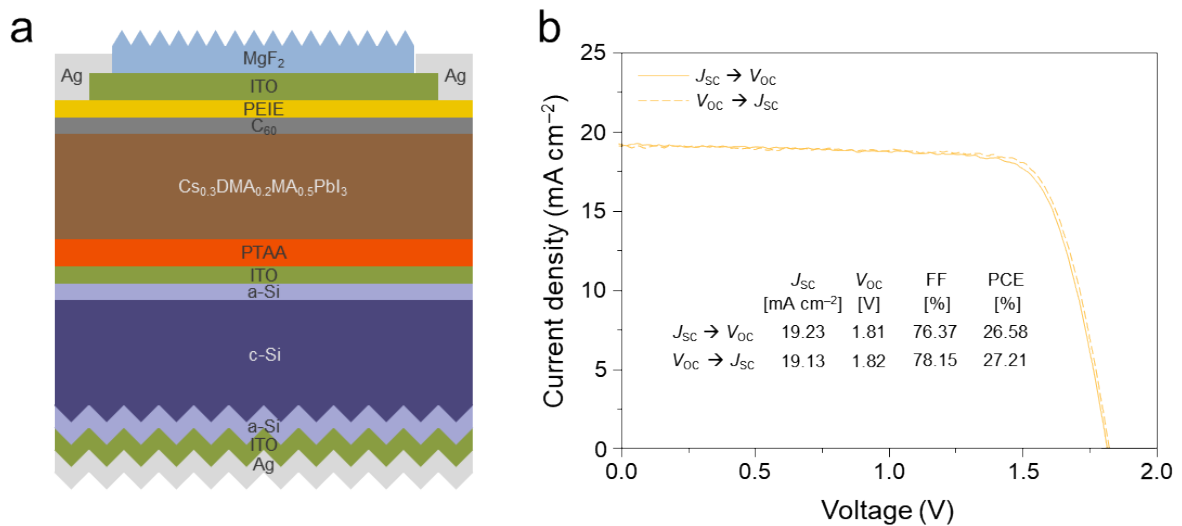


Fig. S17 (a) Schematic illustration and (b) 2 electrode J - V curves of the perovskite/Si tandem solar cell.

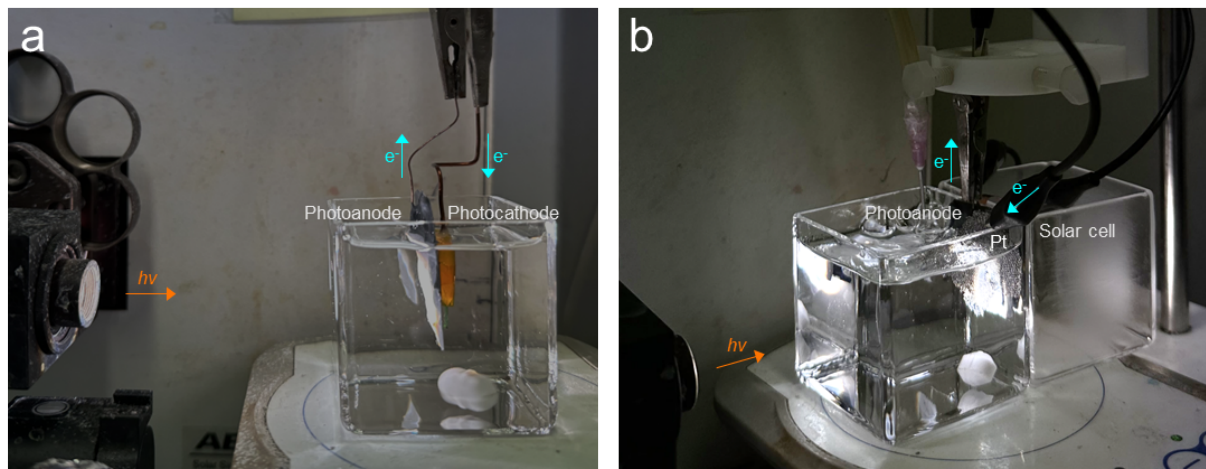


Fig. S18 Photographs of (a) PA-PC and (b) PV-PA tandem devices.

Table S1. Series resistances (R_s), charge transport resistances (R_{sc}), charge transfer resistances (R_{ct}), and chi-squared (X^2) values fitted from EIS curves.

Photoanodes	R_s [$\Omega \text{ cm}^2$]	R_{sc} [$\Omega \text{ cm}^2$]	R_{ct} [$\Omega \text{ cm}^2$]	X^2 [10^{-3}]
NiFeCoO _x /CPF-TCB/Mo:BiVO ₄	4.192	5.525	41.45	6.118
NiFeCoO _x /Mo:BiVO ₄	4.233	36.13	42.65	6.051

Table S2. Donor densities (N_D) of photoanodes calculated by M-S plots

Photoanodes	N_D [10^{20} cm $^{-3}$]
CPF-TCB/Mo:BiVO ₄	2.125
Mo:BiVO ₄	1.438

Table S3. Fitting parameters and chi-squared (χ^2) values of the TRPL.

Photoanodes	A_1 [%]	τ_1 [ns]	A_2 [%]	τ_2 [ns]	τ_{avg} [ns]	χ^2
CPF-TCB/Mo:BiVO ₄	30.32	1.750	69.68	0.2058	0.6740	1.499
Mo:BiVO ₄	44.89	3.899	55.11	0.1455	1.830	2.082

Table S4. STH conversion efficiency benchmarks of PA-PC tandem devices in mode T.

Year	Photoanode	Photocathode	STH [%]	Ref
this work	NiFeCoO _x /CPF-TCB/Mo:BiVO ₄ /SnO ₂	Pt/ITO/SnO ₂ /Perovskite/spiro-OMeTAD/Au	6.75	
2022	NiCoFe-B _i /CPF-TCzB/Sb ₂ S ₃	Pt/TiO ₂ /p-Si/SLG	5.21	¹
2022	RuO ₂ /PDDA/Sb ₂ S ₃ /TiO ₂	Pt/TiO ₂ /p-Si	4.92	²
2021	Co ₄ O ₄ /pGO/BiVO ₄ /SnO _x	Pt/TiO _x /PIP/CuO _x	4.30	³
2018	NiFeO _x -B _i /BiVO ₄	Pt/CdS/CuIn _{0.5} Ga _{0.5} Se ₂ /Mo	3.70	⁴
2021	NiFeO _x /CTF-BTh/Mo:BiVO ₄	MoS _x /CTF-BTh/Cu ₂ O/Au	3.24	⁵
2021	NiFeO _x -B _i /BiVO ₄	Pt/HfO ₂ /CdS/HfO ₂ /Cu ₂ ZnSnS ₄ /Mo	3.17	⁶
2018	NiFeO _x /Mo:BiVO ₄	RuO _x /TiO ₂ /Ga ₂ O ₃ /Cu ₂ O/Au	3.00	⁷
2023	NiFe/Mo:BiVO ₄ /SnO ₂	Pt/TiO ₂ /CdS/Bi ₂ S ₃ /Cu ₃ BiS ₃ /Au	2.33	⁸
2018	NiOOH/FeOOH/Mo:BiVO ₄	NiMo/SiO ₂ /n ⁺ p-Si	2.10	⁹
2021	Co-P _i /BiVO ₄	Pt/TiO ₂ /CdS/Cu ₃ BiS ₃ /Mo	2.04	¹⁰
2020	NiOOH/FeOOH/BiVO ₄	Pt/TiO ₂ /n-Si/TiO ₂ /Ni	1.90	¹¹
2021	NiFe/Mo:BiVO ₄ /SnO ₂	Pt/Ga ₂ O ₃ /CdS/SnS/Au	1.70	¹²

Table S5. STH conversion efficiency benchmarks of PV-PA tandem devices in mode T.

Year	Photoanode	Solar cell	STH [%]	Ref
this work	NiFeCoO_x/CPF-TCB/Mo:BiVO₄/SnO₂	Perovskite/Si	9.0	
2015	Co-P _i /BiVO ₄ /WO ₃	GaAs/InGaAsP	8.1	13
2019	NiOOH/FeOOH/BaSnO _{3-x}	Perovskite	7.9	14
2016	NiOOH/FeOOH/BiVO ₄ // Ni ₂ FeO _x /Fe ₂ O ₃ (dual PA)	2jn c-Si	7.7	15
2021	NiFe/BiVO ₄ /SnO ₂	Perovskite/Si	7.3	16
2016	NiOOH/FeOOH/W,Mo:BiVO ₄ /WO ₃	Dye-sensitized	7.1	17
2023	BiVO ₄ /SnO ₂	Perovskite	7.0	18
2018	2 × NiOOH/FeOOH/BiVO ₄ (dual PA)	Perovskite	6.5	19
2017	NiOOH/FeOOH/Mo:BiVO ₄ /SnO ₂	Perovskite	6.3	20
2016	Ni(OH) ₂ /Fe(OH) ₂ /Mo:BiVO ₄ /SnO ₂	Perovskite	6.2	21
2023	NiFeO _x /BiVO ₄ /In ₂ O ₃	Perovskite/Si	6.1	22
2015	NiOOH/FeOOH/W,Mo:BiVO ₄ /WO ₃	Dye-sensitized	5.7	23
2013	Co-P _i /W:BiVO ₄	2jn a-Si	4.9	24

References

- 1 L. Wang, W. Lian, B. Liu, H. Lv, Y. Zhang, X. Wu, T. Wang, J. Gong, T. Chen, H. Xu, *Adv. Mater.*, 2022, **34**, 2200723.
- 2 Y. S. Park, X. Jin, J. Tan, H. Lee, J. Yun, S. Ma, G. Jang, T. Kim, S. G. Shim, K. Kim, J. Lee, C. U. Lee, S. J. Hwang and J. Moon, *Energy Environ. Sci.*, 2022, **15**, 4725–4737.
- 3 S. Ye, W. Shi, Y. Liu, D. Li, H. Yin, H. Chi, Y. Luo, N. Ta, F. Fan, X. Wang and C. Li, *J. Am. Chem. Soc.*, 2021, **143**, 12499–12508
- 4 H. Kobayashi, N. Sato, M. Orita, Y. Kuang, H. Kaneko, T. Minegishi, T. Yamada and K. Domen, *Energy Environ. Sci.*, 2018, **11**, 3003–3009.
- 5 Y. Zhang, H. Lv, Z. Zhang, L. Wang, X. Wu and H. Xu, *Adv. Mater.*, 2021, **33**, 2008264.
- 6 D. Huang, K. Wang, L. Li, K. Feng, N. An, S. Ikeda, Y. Kuang, Y. Ng and F. Jiang, *Energy Environ. Sci.*, 2021, **14**, 1480–1489.
- 7 L. Pan, J. H. Kim, M. T. Mayer, M. K. Son, A. Ummadisingu, J. S. Lee, A. Hagfeldt, J. Luo and M. Grätzel, *Nat. Catal.*, 2018, **1**, 412–420.
- 8 S. Moon, J. Park, H. Lee, J. W. Yang, J. Yun, Y. S. Park, J. Lee, H. Im, H. W. Jang, W. Yang and J. Moon, *Adv. Sci.*, 2023, **10**, 2206286.
- 9 W. Vijselaar, P. Westerik, J. Veerbeek, R. M. Tiggelaar, E. Berenschot, N. R. Tas, H. Gardeniers and J. Huskens, *Nat. Energy*, 2018, **3**, 185–192.
- 10 D. Huang, L. Li, K. Wang, Y. Li, K. Feng and F. Jiang, *Nat. Commun.*, 2021, **12**, 3795.
- 11 B. Liu, S. Feng, L. Yang, C. Li, Z. Luo, T. Wang and J. Gong, *Energy Environ. Sci.*, 2020, **13**, 221–228.
- 12 H. Lee, J. W. Yang, J. Tan, J. Park, S. G. Shim, Y. S. Park, J. Yun, K. Kim, H. W. Jang and J. Moon, *Adv. Sci.*, 2021, **8**, 2102458.
- 13 Y. Pihosh, I. Turkevych, K. Mawatari, J. Uemura, Y. Kazoe, S. Kosar, K. Makita, T. Sugaya, T. Matsui, D. Fujita, M. Tosa, M. Kondo and T. Kitamori, *Sci. Rep.*, 2015, **5**, 11141.
- 14 M. Kim, B. Lee, H. Ju, J. Y. Kim, J. Kim and S. W. Lee, *Adv. Mater.*, 2019, **31**, 1903316.
- 15 J. H. Kim, J. W. Jang, Y. H. Jo, F. F. Abdi, Y. H. Lee, R. Van De Krol and J. S. Lee, *Nat. Commun.*, 2016, **7**, 13380.
- 16 J. W. Yang, I. J. Park, S. A. Lee, M. G. Lee, T. H. Lee, H. Park, C. Kim, J. Park, J. Moon, J. Y. Kim and H. W. Jang, *Appl. Catal. B*, 2021, **293**, 120217.
- 17 X. Shi, H. Jeong, S. J. Oh, M. Ma, K. Zhang, J. Kwon, I. T. Choi, I. Y. Choi, H. K. Kim, J. K. Kim and J. H. Park, *Nat. Commun.*, 2016, **7**, 11943.
- 18 Z. Xu, L. Chen, C. J. Brabec and F. Guo, *Small Methods*, 2023, **7**, 2300619.
- 19 S. Wang, P. Chen, Y. Bai, J. H. Yun, G. Liu and L. Wang, *Adv. Mater.*, 2018, **30**, 1800486.
- 20 S. Xiao, C. Hu, H. Lin, X. Meng, Y. Bai, T. Zhang, Y. Yang, Y. Qu, K. Yan, J. Xu, Y. Qiu

- and S. Yang, *J. Mater. Chem. A*, 2017, **5**, 19091–19097.
- 21 Y. Qiu, W. Liu, W. Chen, G. Zhou, P. C. Hsu, R. Zhang, Z. Liang, S. Fan, Y. Zhang and Y. Cui, *Sci. Adv.*, 2016, **2**, 1501764.
- 22 M. G. Lee, J. W. Yang, I. J. Park, T. H. Lee, H. Park, W. S. Cheon, S. A. Lee, H. Lee, S. G. Ji, J. M. Suh, J. Moon, J. Y. Kim and H. W. Jang, *Carbon Energy*, 2023, **5**, e321.
- 23 X. Shi, K. Zhang, K. Shin, M. Ma, J. Kwon, I. T. Choi, J. K. Kim, H. K. Kim, D. H. Wang and J. H. Park, *Nano Energy*, 2015, **13**, 182–191.
- 24 F. F. Abdi, L. Han, A. H. M. Smets, M. Zeman, B. Dam and R. Van De Krol, *Nat. Commun.*, 2013, **4**, 2915.